An electrochemical detection of cadmium (II) and lead (II) ions using a polymer-modified electrode with a Schiff base by square wave voltammetry

Mohammed Qasim Mohammed (mahammed.qasim@uobasrah.edu.iq)
University of Basrah https://orcid.org/0000-0003-4998-0647
Hani Khalil Ismail
Hasan Fisal Alesary
Stephen Barton

Research Article

Keywords: Square wave voltammetry, electrochemical detection, conducting polymers, modified electrode poly(3,4-ethylenedioxythiophene), Schiff base

Posted Date: February 25th, 2021

DOI: https://doi.org/10.21203/rs.3.rs-240222/v1

Abstract

The work herein concentrates on the electrochemical detection of heavy metal ions, specifically cadmium and lead ions. The introduction and modification of functional groups such as Schiff bases had led to an enhanced sensitivity of the electrode to analytes. In this study, a platinum electrode has for the first time been modified with poly(3,4- ethylenedioxythiophene) (PEDOT/Schiff base) in CH2Cl2 containing Bu4NPF6 for use to detection cadmium (II) and lead (II) ions. The structure and morphology of the polymer coatings were characterised by Fourier transform infrared (FTIR) spectroscopy and scanning electron microscopy (SEM), respectively. The electrochemical synthesis and redox state response in monomer-free synthesised films have been studied by cyclic voltammetry. Moreover, the effect of scan rate on the electrochemical behaviour of the modified electrodes was also studied. The voltammetric findings have been used to calculate the surface coverage required for the polymer films and the stability of polymer electrodes in the monomer-free solutions. Square wave voltammetry (SWV) was applied for the determination of cadmium (II) and lead (II) ion concentrations and to assess the effects of pH on aqueous samples. The limits of detection for the modified electrode for cadmium (II) and lead (II) were found to be 0.95 µg L-1 and 1.84 µg L-1, respectively. These findings revealed that modified films can be considered good candidates for application in electrochemical detection devices

Introduction

Globally, pollution of the planet is one of most vital problems because of the widespread and critical damage such pollution can cause [1-3]. Heavy metal ions like Cu, Hg, Zn, Pb, Ni, and Cd are considered toxic even in extremely low concentrations [3]. These metal ions can cause significant harm and damage in human organs such as the kidneys, liver, brain and the lungs and respiratory system [4]. Recently, contamination from heavy metals has become a significant problem as a result of the rapid development of industrial activities [5]. Contamination of the environment, especially with cadmium (II) and lead (II) ions, poses a real danger to human health because these ions are toxic, non-biodegradable, and accumulate in the body [6, 7]. According to World Health Organization (WHO), the maximum permitted concentrations of cadmium (II) and lead (II) in drinking water are 5 µg L^{-1} and 50 µg L^{-1}, respectively [8]. Thus, it becomes necessary to find fast, sensitive, and selective methods for the detection of cadmium and lead in various sample types. There have been several reports of electrochemical methods used to detect cadmium (II) and lead (II) [9] and these methods have many positive features compared with other techniques such as quick analysis time, simple inexpensive technology and high sensitivity [10, 11].

The key factor in electrochemical voltammetry methods is the manufacture and usage of electrode surfaces that facilitate an electrical potential between the electrode surface and solution interfaces. Polymerisation and chemical adsorption can enhance the analytical functional performance of an electrode, in areas such as the sensitivity and selectivity of analytes. A range of diverse materials, such as functionalized graphene oxide, carbon nanotubes [12] and polymer films, have previously been used in voltammetric methods for the detection of metal ions.

Electroactive polymers such as polypyrrole [13], polyaniline [14], poly(3,4-ethylenedioxythiophene) (PEDOT) [15] and their derivatives have high intrinsic conductivities and have been intensively studied to date [16]. These materials have a key role in electrocatalysis, energy storage, and electrochemical sensors because of their unique properties such as stability, flexibility, simple synthetic processes and low cost [17]. In addition, these species have a good congruence with biomolecules. Therefore, these substances have become an effective alternative to many materials used in, for example, batteries, chemical sensors, corrosion inhibitors, actuators, and in medical engineering. Recently, electroactive polymers have been used in the production of promising chemical sensor devices [18]. Chemical modification and the preparation method, can often be manipulated to achieve the desired mechanical and electrochemical features of these polymers. Thus, electroactive polymers play a vital role in analytical fields and the fabrication of chemical sensors [19]. A significant advantage of detection devices based on conjugated polymers is that they have the potential to show sensitive and selective properties and fast responses. In recent years, the fabrication of functionalized polymer electrodes has played a critical role in the production of a novel generation of electroanalysis systems with improved sensitivities and selectivities [20]. Several electrochemical tools based on polymers have been developed for use as detectors for chemical pollutants [21].

Modified electrodes in electroanalytical chemistry offer an easy and appropriate technology for examining the reactions of various substrates, and inorganic, organic, and biological species [3, 22]. The chemically modified polymer electrode can be prepared and controlled using electrochemical techniques that allow for the generation of a thin synthetic polymer film [23]. In modern electroanalytical devices, analytical performance in areas such as sensitivity, selectivity, and stability was dependent on electrode composition due to the straightforward working mechanism and fast responses achieved [7]. Various modes can be used including square wave voltammetry (SWV), which is considered a perfect candidate for sensitivity and quantification of various species such as alkaloids, phenols, vitamins, pesticides, herbicides and fungicides, benzoquinones, proteins, terpenoids, drugs and heavy metals [24, 25]. Among diverse electroactive polymers, poly(3,4-ethylenedioxythiophene) (PEDOT) is of particular interest in the area of chemical sensing due to its high conductivity and good environmental stability compared with other electroactive polymer families. Electropolymerisation of EDOT can be accomplished through the oxidation of the EDOT monomer in the presence of appropriate counter-ions. Schiff bases have emerged as potential chemical detectors for many of the metal ions of general interest as they can selectively bind to specific cations [26]. Current research aims to enhance the sensitivity and selectivity of modified polymer electrodes to be more efficient with regard to metal ion determination and with improved stability, repeatability and conductivity of the electrodes [27, 28]. The goals of this project were: (i) to electropolymerise and modify a PEDOT/Schiff base electrode in non-aqueous medium; (ii) to examine the response of the prepared modified polymer electrode using CV; (iii) to study the effect of scan rate; and (iv) to investigate the interaction of the polymer electrode with heavy metal ions, in particular Cd (II) and Pb (II) ions, using square wave voltammetry (SWV).

Experimental

Materials and reagents

2-aminomethyl-3,4-ethylenedioxythiophene (EDOT-MeNH_2) was prepared using the following procedure [29]. Chloromethyl-3,4-ethylenedioxythiophene (EDOT–MeCl), salicylaldehyde (98%), potassium phthalimide and hydrazine hydrate were obtained from Sigma Aldrich. Dichloromethane (DCM) (CH_2Cl_2, AR; Tianjin Damao Chemical Reagent Factory) was purified by distillation over calcium hydride before use. Tetrabutylammonium hexafluorophosphate (Bu_4NPF_6, 99%; Acros Organics) was dried under vacuum at 60 ºC for 24 h before use. An acetate buffer solution was prepared by adjusting 0.2 M sodium acetate (Aldrich) to the desired pH through the addition of 0.2 M glacial acetic acid. All the processes performed in aqueous media and the preparation of the aqueous solutions was carried out using ultra-pure quality water.

Instrumental

Cyclic voltammetry (CV) and square wave voltammetry (SWV) were performed with a PGSTAT20 potentiostat/galvanostat from ECO-Chemie (Utrecht, The Netherlands). The Pt (1 mm) electrodes was polished by using 0.3 µm alumina and then washed with pure water. The electrodeposition of EDOT-Schiff (monomer) base on the Pt electrode was achieved via cyclic voltammetry. Square wave voltammetry measurements were obtained via a potentiostat device which contained three electrodes: an Ag/AgCl reference electrode, a platinum plate (2 mm^2) counter electrode, and a PEDOT-Schiff base/Pt working electrode. FTIR spectra were recorded to confirm the chemical composition of the films using a Perkin Elmer FTIR Frontier spectrophotometer (Waltham, USA). Scanning electron microscopy (FEI SIRION SEM) was performed to examine the surface morphology of polymer film deposited on the Pt substrate. Cyclic voltammetry was used for the electrochemical polymerization of EDOT/Schiff base. The voltage range was swept 10 times between 0.5 to 1.4 V at various scan rates (10, 20, 30, 50 and 100 mV s^{-1}). The formation of the polymer layer on the surface of the electrode was evidenced by the emergence of a dark colouration on the working electrode. The coated polymer film was washed using deionized water to eliminate the excess monomer from electrode surface, which was then dried at room temperature.

Preparation of stock solutions

Standard solutions (100 ppm) of each metal ion were synthesised by dissolving ion metal in ultrapure deionized water. The lead standard solution was prepared by dissolving 0.1598 g of $Pb(NO_3)_2$ (99.9%, Aldrich) in deionized water and diluting to 1 litre. The cadmium solution was produced by dissolving 0.274 g of $Cd(NO_3)_2.4H_2O$ (99.9%, Aldrich) in ultrapure deionized water and diluting to 1 litre. These stock solutions were used to prepare a series of different concentrations from 5 to 100 ppm for each of the metal ions.

Preparation of (2,3-dihydrothieno[3,4-b][1,4]dioxin-2-yl)methanamine PEDOT/NH_2 [29]

The original monomer of EDOT–NH_2 was synthesised as illustrated in Scheme 1. The substitution of the chloride group by an amine group was achieved via a Gabriel reaction in the presence of potassium

phthalimide and hydrazine. A mixture of 2-(chloromethyl)-2,3-dihydrothieno[3,4-b][1,4]dioxine (0.3 g, 1.6 mmol) and potassium phthalimide (0.4 g, 2.2 mmol) were dissolved in 10 ml of dimethylformamide and heated at 100 ºC for 24 h. Next, the product was decanted into 100 ml of water and extracted with chloroform. 0.1 M sodium hydroxide and water were used to wash the organic layer and then dried with $MgSO_4$. After this step, the product was mixed with hydrazine hydrate (0.16 g, 3.2 mmol) and the mixture added to 10 ml of methanol and heated to 50 ºC for 1 h. After the reaction had stopped, water was added to the mixture and the solvent was extracted under vacuum. This mixture was acidified with HCl and heated to 60 ºC for 1 h. Next, the neutralisation step was accomplished for this solution using 2 M sodium hydroxide. After solvent evaporation, the amine compound was purified by column chromatography (silica gel; eluent: methanol/ dichloromethane 1:4).

Preparation of PEDOT/Schiff ligand [30]

2-aminomethyl-3,4-ethylenedioxythiophene (EDOT– $MeNH_2$) (0.55 g, 2 mmol) and salicylaldehyde (0.24 g, 2 mmol) was dissolved in 20 ml of methanol with 2-3 drops of acetic acid as a catalyst under continuous stirring and was refluxed for 5 h [30]. The reaction was monitored via thin-layer chromatography. At the end of the reaction, the solution obtained was filtered and washed with methanol. The crude product was dried and purified by crystallization from ethanol. The synthesis of the monomer and polymerisation reaction steps is illustrated in Scheme 1.

Electropolymerisation of EDOT/Schiff base

The EDOT derivative which was synthesised using a condensation reaction with the aldehyde EDOT-Schiff base and electropolymerised in suitable solution to create the conducting polymer. For voltammetric deposition experiments, the EDOT/Schiff base was electropolymerized on the Pt electrode from a solution of 10 mM EDOT/Schiff base with 0.1 M tetrabutylammonium hexafluorophosphate (Bu_4NPF_6) in DCM using voltage cycling between 0.5 V and 1.4 V vs. the reference electrode (Ag/AgCl). The PEDOT/Schiff base film was grown on the Pt surface for 10 sequential scans with increasing anodic and cathodic peak current densities. The modified polymer electrode is hereafter referred to as the PEDOT/Schiff base.

Electrochemical detection of metal ions

Electrochemical measurements were performed with an AUTOLAB Analyser using a cell with three electrodes as described above. The working electrode was a PEDOT/Schiff base electrode, the reference electrode an Ag/AgCl/ 3M KCl electrode and the auxiliary electrode a platinum electrode. Acetic acid/sodium acetate (0.2 M CH_3COOH + 0.2 M CH_3COONa) buffer solutions (pH 2-6) containing different concentrations of cadmium (II) and lead (II) ions were used as the electrolytes for all measurements. All experiments were conducted at ambient temperature, 25 ± 2 ºC. Square wave voltammetric parameters were as follows: initial potential -0.5 V, end potential 1.5 V, pulse amplitude 10 mV.

Results And Discussion

Electrochemical formation of PEDOT/Schiff

The poly(EDOT-Schiff base) film was prepared potentiodynamically with a voltage ranging between − 0.50 V and 1.40 V over ten scans from a 0.1 M solution of monomer in CH_2Cl_2 containing Bu_4NPF_6 onto a Pt electrode at a scan rate of 10 mV s^{-1} at 25 ± 2 ºC. **Fig. 1** illustrates the cyclic voltammograms that were recorded during the synthesis of poly(EDOT-Schiff base). As shown in **Fig. 1,** the onset of the oxidation potential for the PEDOT-Schiff base film was 1.22 V. During polymerization, a black-coloured layer of polymer film formed on the Pt electrode. The current peak of the polymer film increased with increasing number of cycles, which corresponds to the systematic growth of the polymer film on the Pt electrode [31]. The cyclic voltammogram in **Fig. 1** shows a nucleation loop in the first cycle where this anodic current related to the oxidation of the monomer and nucleation of poly(EDOT/Schiff) [32]. The nucleation loop vanished in the following cycles because of the persistent growth of the film preventing further nucleation in the subsequent scans. The redox processes of poly(EDOT/Schiff) has led to the emergence of anodic and cathodic peaks at 0.53V and -0.07 V, respectively, in the cyclic voltammogram. Moreover, the increase in redox peak current values in the voltammogram implies that the amount of electrodeposited PEDOT polymer has increased on the Pt electrode, which led to an increased thickness of the deposited polymer [33]. In addition, two peaks probably indicate the potential peaks of the monomers, which depended on the type and of size the anion present in the reaction medium. In other words, the emergence of redox peaks in the voltammogram can be significantly influenced by the nature and size of the ionic species present in the electrolyte.

Fig. 2 shows the cyclic voltammogram (scan 10) of the electropolymerisation of the (EDOT/ Schiff) monomer at various scan rates ranging from 5 - 100 mV s^{-1} under the same polymerisation conditions used for the voltammogram in **Figure 1.** The molar coverage of polymer films per unit area can be calculated from the amount of charge of the last scan of the deposited polymer using Faraday's law and **Eq. 1** [34].

See formula 1 in the supplementary files.

Here, *F re*presents the Faraday constant (C mol^{-1}), Γ is the molar coverage (mol cm^{-2}), *A* is the modified electrode area (cm^2), *Q re*presents the cathodic charge and *n* is the number of electrons involved in the electropolymerisation. Herein, *n* is equal to 2.3 [35] and the modified electrode has a surface area of 0.00785 cm^2. The molar coverage is applied to estimate the thickness of the polymer surface (*h*/µm) using **Eq. 2 and 3** [36].

See formula 2 in the supplementary files.

See formula 3 in the supplementary files.

Here, *c* and ρ are the concentration and density of the monomer, respectively, and *Mr* is the molecular mass of the monomer (273.3 g/mol). *h* is the thickness of polymer film. The relative standard deviation

(RSD%) from three consecutive experiments was calculated, as shown in **Table 1**, which also reports the cathodic charge, surface coverage and thickness of prepared polymer films.

Table 1 Charge of reduction peak of poly(EDOT/Schiff) at different scan rates (5-100 mV s^{-1}). Electrode area was 0.00785 cm^{-2}.

Polymer films	Scan rate (mV s^{-1})	Charge of reduction peak *Q* (C)	RSD% n=3	Coverage *Γ* (mol cm^{-2})	Thickness *h* (µm)
poly(EDOT/Schiff)	10	1.30×10^{-2}	1.32	7.46×10^{-6}	14
20	1.12×10^{-2}	2.45	6.42×10^{-6}	12	
30	9.15×10^{-3}	1.85	5.25×10^{-6}	10.5	
50	8.02×10^{-3}	2.06	4.60×10^{-6}	9.22	
100	6.11×10^{-3}	1.47	3.50×10^{-6}	7.01	

Electrochemical characterisation of polymer films

In order to obtain a greater insight into the electrochemical behaviour and stability of the polymer films, the electrochemical features were analysed carefully using cyclic voltammetry in a background electrolyte (monomer-free) of dichloromethane and aqueous solution-Bu_4NPF_6 (0.1 M) for polymer film which was prepared using a scan rate of 10 mV s^{-1} (**Fig. 1**), as depicted in **Fig. 3A** and **3C,** respectively. Voltammetric study findings have shown broad redox current peaks which can probably be attributed to the counterions diffusing into the chain polymer film for both electrolytes [20]. The voltammogram of poly(EDOT/Schiff) films exhibit a broad positive peak at 0.61 V vs. Ag/AgCl and a negative peak at 0.08 V vs. Ag/AgCl in DCM electrolyte. On the other hand, a broad positive peak appears at 0.52 V vs. Ag/AgCl and a negative peak at 0.16 V vs. Ag/AgCl in aqueous electrolyte, which are representative of the oxidation and reduction of the film produced, respectively. Herein, we observed a decrease in the peak currents as a function of

increasing scan number; thus, there is decay in the peak potentials and associated CV shapes were changed. This could be attributed to degradation of the film when switching to the overoxidation potential, which led to poor stability during redox cycling.

In this work, the effect of scan rate on electrochemical response has been studied in a background electrolyte (monomer-free) of dichloromethane and aqueous solution-Bu_4NPF_6 (0.1 M), as shown in **Fig. 3B** and **Fig. 3D**. From these two curves, we can observe that the current of the peak was proportional to the scan rate [37]; this property supports the assumption of good electro-activity and stability of the polymer film. This finding indicates that redox current peaks are proportional to the scan rates for the same polymer electrode [38]. Further, both oxidation and reduction peaks have a linear relationship with scan rate, which is indicative of surface-confined control, as revealed in **Figs. 4A** and **4B**. **Tables 2** and **3** show charges for the electrochemical response of polymer growth in **Fig. 1** as cycled in the background electrolyte (monomer-free) at different scan rates, as presented in **Fig. 3B** and **3D**. The charge was calculated from the CV curves in **Fig. 3B** and **3D** by integration of the current of the redox peaks with respect to time. The charges found for cycles 1 and 10 are shown in **Tables 2** and **3**.

Table.2 Cathodic charge values of PEDOT/Schiff panels in **Figure 1** exposed to 0.1 M Bu_4NPF_6 in DCM electrolyte (monomer-free) at various scan rates.

Scan rate mV s^{-1}	***Q* red, 1st cycle C**	***Q* red, 10th cycle C**	**% *Q* red 10th / *Q* red 1st retention**
10	8.45×10^{-3}	6.12×10^{-3}	72
20	5.89×10^{-3}	4.78×10^{-3}	81
30	4.78×10^{-3}	3.96×10^{-3}	82
50	4.08×10^{-3}	3.08×10^{-3}	75
100	2.64×10^{-3}	2.25×10^{-3}	85

Table.3 Cathodic charges of PEDOT/Schiff panels in **Figure 1** exposed to 0.1 M Bu_4NPF_6 in aqueous electrolyte (monomer-free) at various scan rates.

Scan rate mV s^{-1}	*Q* red, 1st cycle C	*Q* red, 10th cycle C	% *Q* red 10th / *Q* red 1st retention
10	8.19 × 10^{-3}	6.12 × 10^{-3}	77
20	3.71 × 10^{-3}	3.08 × 10^{-3}	83
30	2.97 × 10^{-3}	2.68 × 10^{-3}	90
50	2.13 × 10^{-3}	2.45 × 10^{-3}	87
100	1.86 × 10^{-3}	1.70 × 10^{-3}	91

FTIR characterisation of EDOT/NH_2 and PEDOT/Schiff base structures

Fig. 5 illustrates the FTIR spectra of EDOT/NH_2 and electrochemically prepared poly(EDOT/Schiff base) structures. An FTIR spectrum of PEDOT/NH_2 has the distinctive features of PEDOT and the amino group. The bands of the NH_2 group vibrations were observed in the range 3380 - 3240 cm^{-1}. The peaks at 3090 cm^{-1} and 2975 $^{-1}$ cm were assigned to C–H aromatic and C–H aliphatic stretches, respectively. The vibrations for the C-O-C and C-S groups in EDOT were observed at 1100 cm^{-1}, 940 cm^{-1} and 615cm^{-1}, respectively. The bands at 1641, 1535 and 1362 cm^{-1} were attributed to the C=C and C-C stretches in the thiophene cycle. The FTIR spectrum of the prepared polymer Schiff base had characteristics peaks at 1645 cm^{-1} and 3365 cm^{-1} that could be attributed to the imine group (C=N) and OH group, respectively. The band at 2939 cm^{-1} was assigned to the C–H aromatic and dioxyethylene bridge stretching modes of the EDOT molecule. Further, the bands at 1128 cm^{-1} and 975 cm^{-1} were noted for EDOT/Schiff [37, 38].

Morphological characterisation of PEDOT/Schiff base

Properties of electroactive polymers such as activity and stability are closely related to surface morphology. The surface morphology of the PEDOT-Schiff film electrodeposited on the Pt electrode was

examined by scanning electron microscopy (SEM), as shown in **Fig. 6**. The polymer film was preformed potentiodynamically by applying the potential range −0.5 to 1.5 V vs. Ag/AgCl using a scan rate of 10 mV s^{-1} and 100 mV s^{-1} for 10 cycles. The surface film clearly exhibits growth processes on surface whereby the existence of a number of small globules and clusters which are linked together like chains can be observed. These electrode surfaces have uniform nanostructures and compactness. In general, the morphology of the polymer surface is highly affected by the conditions of the experiment such as the pH, temperature, solvent type, ions present, and scan rates [39]. SEM micrographs of PEDOT/Schiff electrodes at different scan rates are shown in **Fig. 6**. SEM images indicated that different scan rates result in a change of primary particle size. It was observed that the film prepared at 100 mV s^{-1} (**Fig. 6B**) has smoother structure with fused particles (grain sizes on the order of a few micrometres) compared to the film prepared at 10 mV s^{-1}, which has a much more globular morphology, having grain sizes in the order of nanometres ranges (**Fig. 6A**).

These variations in the surface morphology can be attributed to the fast and slow nucleation and growth rate of the polymer which is affected by timescale. At high scan rate, the nucleation and growth rate of the polymer are fast (instantaneous nucleation reaction). As a result, the redox system does not maintain an equilibrium state during the potential scan, producing larger and different crystal sizes of morphology. In contrast, at slow a scan rate, equilibrium processes and progressive nucleation is predominant. Therefore, the movement of neutral species is slower than the movement of charged species, forming highly homogeneous crystal sizes of morphology.

The Influences of pH

It is unquestionable that pH is one of the parameters which directly influence the voltammograms' shapes, and then it is significant to study the effect of pH on electrochemical processes. This process aims to reach to the highest peak current during experiments [40, 41]. Analyte solution containing 5 µg L^{-1} of Cd (II) and Pb (II) ions in media with different pH values were used for the voltammetric investigation. The square wave voltammograms exhibited clear peaks for metal ions in media with diverse pH values. It was found that the peak current shapes and heights in solution of pH 5 were well-defined and higher compared to other pH values. Thus, pH 5 was considered suitable for determination of ion concentrations in solution. The findings obtained are graphically depicted in **Fig. 7** where, as shown, the modified electrodes have low current peaks in highly acidic solution (pH 2) and after which the current peak increases with increasing pH until it reaches 5, at which we have tested for cadmium and lead cations.

Measurement of Cd (II) and Pb (II) using SWV

The procedure for the voltammetric measurements for the electro-analytical determination of cadmium and lead concentrations in aqueous solution was divided into two steps. Firstly, the modified electrode was immersed in sample solution containing the analyte (Cd (II) or Pb (II)) at a known pH=5 and a selected concentration (5-100 µg L^{-1}), where metal ions were binding chemically to the ligands at the surface of the electrode; and secondly, the polymer electrode was removed from the metal ion solution

and rinsed with deionized water, and then transferred to a voltammetric cell containing only a supporting electrolyte (acetate buffer solution). The square wave voltammograms were performed using different cadmium and lead concentrations. **Fig. 8** shows the proposed interaction between the polymer ligand and metal ions.

The determination of Cd (II) and Pb (II) ions

Optimal practical conditions for the determination of Cd (II) and Pb (II) ions by the PEDOT/Schiff electrode using the SWV technique, were assessed separately for each electrode. Initially, the current responses were recorded for the polymer electrodes using a blank solution without metal ions. The blank solution responses do not have any current signals in the voltage range from −1.2 to 0 V, as illustrated in **Fig. 9** (black line). Accumulation of the Cd (II) and Pb (II) ions occurred by immersion of the modified electrode in buffer solution at pH 5 containing Cd (II) and Pb (II) ions. This process led to complex formation between the metal ions and the PEDOT/Schiff base layer. The chemical accumulation process which occurred for Cd (II) and Pb (II) ions probably affected the accumulation of other reducible species at the voltage used during the preconcentration processes. After the immersion of metal ions in the PEDOT/Schiff electrode, they were washed with pure water. After that, the modified electrode was moved to the electrochemical cell which contained buffer solution. The SWV response was registered for each metal ion, i.e. Cd (II) and Pb (II) [42, 43].

The square wave voltammograms of modified electrodes, after 15 min of immersion in buffer solution, at pH 5 with 5 μg L^{-1} of Cd (II) and Pb (II) ions, are shown in **Fig. 9**. The determination of Cd (II) and Pb (II) ion concentrations was investigated between −1.2 to 0.0 V (vs. Ag/AgCl). As can be noted in **Fig. 9**, the interaction of the Cd (II) and Pb (II) ions with the modified electrode surface leads to the alteration of the electrochemical properties of the electrode. Clearly, the anodic peak has increased due to Cd (II) and Pb (II) ions, which formed a complex on the modified electrode (**Fig. 9**), compared with the peak current recorded after immersion of the same electrode in solution without metal ions (**Fig. 9**, **A** and **B**). The calibration equations and correlation coefficients (R^2) were calculated for the Cd (II) and Pb (II) ions as $y = 1.639 + 0.434x$ (x: μg L^{-1}, y: μA), $R^2 = 0.9989$ for Cd (II) and $y = 0.492 + 0.159x$, $R^2 = 0.9961$ for Pb (II), respectively, as shown in **Fig. 10**. The limits of detection (LOD) were measured as 0.95 μg L^{-1} and 1.84 μg $L^{-1}$for the Cd (II) and Pb (II) ions, respectively, which demonstrates the high sensitivity of the modified polymer electrode towards heavy metal ion detection. The separation in peaks locations for metal ions offer an accurate strategy to detect Cd (II) and Pb (II) ions, significantly reducing interfering effects from other heavy metal ions [44, 45].

Calibration was achieved for the determination of metal ions at pH 5 in buffer solution. **Fig. 10** shows square wave voltammograms recorded using consecutive additions of ion metals over the 5-100 μg L^{-1} concentration range at the EDOT/Schiff modified electrode. Peak currents appeared at -0.77 V and -0.50 V for the various concentrations of Cd (II) and Pb (II), respectively (**Fig. 9**). A linear relationship between the concentration ion metals and current peaks was evident from the experimental findings.

Simultaneous electrochemical determination of Cd (II) and Pb (II) in a binary mixture

The analytical signal of various concentrations of Cd (II) and Pb (II) ions is illustrated in **Figs. 9A** and **9B**, respectively. Subsequently, the simultaneous determination of Cd (II) and Pb (II) ions with the PEDOT/Schiff electrode was carried out to detect Cd (II) and Pb (II) ions in the same solution[46]. SWV voltammograms of the PEDOT/Schiff electrode after sequential additions of different concentrations of Cd (II) and Pb (II) are shown in **Fig. 11**. The characteristic peaks of Cd (II) and Pb (II) were seen at −0.77 and −0.50 V, respectively. These findings were in agreement with the individual species' characteristics (**Fig. 9**). The effects of ion concentrations were examined under optimum conditions. Determination of metal ion concentrations was examined between −1.2 to 0.0 V (vs. Ag/AgCl) at different concentrations such as 5 μg L^{-1} and 100 μg L^{-1} for Cd (II) and Pb (II), respectively. **Fig. 11** represents the square voltammograms recorded at the PEDOT/Schiff electrode with scan rate of 5 mV s^{-1}. From this figure, it can be seen that the individual peak currents increased linearly with increasing concentrations of the individual metal ions in the binary solutions [38].

The findings of the study confirmed that the modified electrode shows the appropriate reliability and efficiency to be used for detecting Cd (II) and Pb (II) ions. Furthermore, the analytical performances of the PEDOT/Schiff electrode in this project was compared with previous work in the literature for Cd (II)) and Pb (II) detection, as illustrated in **Table 4**.

Table 4 Comparison of the analytical performance of PEDOT/Schiff electrode with other modified electrodes.

Electrodes	Methods	Analytes	Detection limit	References
5-Br-PADAP	ASV	Pb (II)	0.1 μg L^{-1}	[12]
P1,2-DAAQ	SWASV	Cd (II)	0.3 μg · L^{-1}	[40]
Pb (II)	0.58 μg · L^{-1}			
GC/ p-1,8-DAN	SWV	Cd (II)	19 ng.L^{-1}	[46]
Pb (II)	30 ng.L^{-1}			
CNFs	ASV	Cd (II)	0.38 μg·L^{-1}	[47]
Pb (II)	0.33 μg·L^{-1}			
polyamide 6/ Chitosan	SWV	Cd (II)	0.88 μg · L^{-1}	[48]
PMTB	DPV	Cd (II)	0.35 μg L^{-1}	[49]
Pb (II)	0.18 μg L^{-1}			
polyaniline	SWASV	Cd (II)	4.43 μg L^{-1}	**[50]**
Pb (II)	3.30 μg L^{-1}			
Poly(1,5-DAN)/MWCNTs	SWASV	Cd (II)	3.2 μg L^{-1}	[51]
Pb (II)	2.1 μg L^{-1}			

Reactivation of PEDOT/Schiff electrode

Repeated usage of the modified electrode to determination of metal ions necessitates the regeneration of the PEDOT/Schiff electrode. Reactivation of PEDOT/Schiff electrode was achieved by immersing the electrode in 0.1 M EDTA solution for 15 min and then washing with ultra-pure water. A voltammogram recorded for PEDOT/Schiff electrode after reactivation was nearly congruous with the voltammogram curve of the PEDOT/Schiff electrode when reacted with metal ions, as shown in **Fig. 12** (red curve). This result indicates that the incorporated metal ions had been totally removed from the PEDOT/Schiff electrode. Therefore, the reactivated PEDOT/Schiff electrode could be applied for the detection of metal ions without any appreciable effect on the electro-activity.

Repeatability and reproducibility study

The repeatability of the PEDOT/Schiff electrode was determined under the optimized conditions using 20 μg L^{-1} Cd (II)) and Pb (II), respectively. Five consecutive measurements were taken using the same polymer electrode; the estimated relative standard deviations (RSD) were 3.4% and 2.8% for Cd (II)) and Pb (II), respectively. Moreover, the reproducibility of the PEDOT/Schiff electrode was examined. This process required the preparation of five modified electrodes which were then used in the detection of 20 μg L^{-1} Cd (II) and Pb (II), respectively. The RSD of the PEDOT/Schiff electrode was 3.8% and 3.1% for Cd (II)) and Pb (II), respectively, which indicated that the PEDOT/Schiff electrode prepared has good repeatability and reproducibility.

Interference study

To assess the selectivity of the modified electrode for the detection of metal ions, the effect of other ions on the response of Cd (II) and Pb (II) was investigated. In this study, various ions were chosen to act as interfering ions to investigate the selectivity of the PEDOT/Schiff electrode. Different ions (Na^+, K^+, Ca^{2+}, Mg^{2+}, Ba^{2+}, Cu^{2+}, Hg^{2+}, Al^{3+}, Fe^{3+}, NO_3^- and Cl^-) were added to a solution containing 20 μg L^{-1} Cd (II) and Pb (II). Addition of interfering ions did not lead to any perceptible difference in measurements, and these findings demonstrated that the electrochemical responses for Cd (II) and Pb (II) were not influenced by the interfering ions in any apparent way.

The interference experiments proved that additive ions have no perceptible interference effect to detection of target ions even when their concentrations exceeds those ion of interest in the solution, at 20 μg L^{-1} Cd (II) and Pb (II), by 50-fold. However, a 30-fold concentration of Fe^{3+}, Cu^{2+} and Hg^{2+} were found to have a slight influence on the determination of Cd (II) and Pb (II) concentrations. The intermetallic compounds which can form between metal ions is a general problem in voltammetric methods, though this small change could be due to competition between iron and the target metal ions for active sites on the surface modified electrode.

Table 5 Three interference analyses for various metal ions on the current response of Cd (II) and Pb (II)

Interfering ions	Relative current change %	
Cd (II)	**Pb (II)**	
Na	0.19	0.25
K	0.36	0.42
Ca	-0.92	-0.85
Mg	1.17	1.09
Ba	1.67	1.35
Cu	6.34	5.92
Hg	-4.93	-5.62
Al	-0.56	-0.54
Fe	5.21	4.12
NO_3	0.47	0.85
Cl	0.78	0.23

Conclusions

The goal of this study was to modify functionalised polymer films for application as electrochemical detection of metal ions in solution. The preparation of polymer films and overall operational performance was monitored using electrochemical (“iVt”) techniques. All modified electrodes were characterised using electrochemical (CV) and spectroscopic (FTIR) techniques. The findings indicated the successful formation of polymer films using cyclic voltammetry. Following the electropolymerisation, films were investigated using various scan rates (10 - 100 mV s^{-1}) to examine electrochemical stability, demonstrating that redox peak currents are linearly dependent on scan rate. Further, the voltammetric data was used to estimate the surface coverage of the polymer films via Faraday’s law. A novel electrochemical tool for metal ions, using electroactive polymer, was developed. PEDOT functionalized with a Schiff base was electrodeposited on a Pt surface electrode by electrochemical techniques (CV) and then used for the detection of Cd (II) and Pb (II) ions in solution. The poly(EDOT/Schiff) electrode exhibited good sensitivity during electro-determination of trace amounts of metal ions (Cd (II) and Pb (II)), showing low limits of detection of 0.95 µg L^{-1} for Cd (II) and 1.84 µg L^{-1} for Pb (II). Cd (II) and Pb (II) ions were detected individually as well as simultaneously using square wave voltammetry using the new poly(EDOT/Schiff) moieties.

Declarations

Acknowledgement

The authors would like to thank the Universities of Basrah, Koya and Kerbala for providing the required materials and instruments for this work.

Declaration of Competing Interest

The authors declare that they have no known competing financial interests or personal relationships that could have appeared to influence the work reported in this paper.

References

1. H. Huang, W. Zhu, X. Gao, X. Liu, and H. Ma, Anal. Chim. Acta **947**, 32 (2016).
2. S. Intarakamhang, W. Schuhmann, and A. Schulte, J. Solid State Electrochem. **17**, 1535 (2013).
3. M. Kamac, I. Kaya, J Inorg Organomet Polym. **25**, 1250 (2015).
4. Y. Lu, X. Liang, C. Niyungeko, J. Zhou, J. Xu, and G. Tian, Talanta **178**, 324 (2018).
5. S. Muralikrishna, D. H. Nagaraju, R. G. Balakrishna, W. Surareungchai, T. Ramakrishnappa, and A. B. Shivanandareddy, Anal. Chim. Acta **990**, 67 (2017).
6. Y. Yao, H. Wu, and J. Ping, Food Chem. **274**, 8 (2019).
7. G.I Dzhardimalieva, I.E. Uflyand, J Inorg Organomet Polym. **28**, 1305 (2018).
8. M. B. Gumpu, S. Sethuraman, U. M. Krishnan, and J. B. B. Rayappan, Sensors Actuators B Chem. **213**, 515 (2015).
9. Z. Xu, X. Fan, Q. Ma, B. Tang, Z. Lu, J. Zhang, G. Mo, J. Ye, and J. Ye, Mater. Chem. Phys. **238**, 121877 (2019).
10. Y. Li, G. Ran, G. Lu, X. Ni, D. Liu, J. Sun, C. Xie, D. Yao, and W. Bai, J. Electrochem. Soc. **166**, B449 (2019).
11. J. Han, J. Yu, Y. Guo, L. Wang, and Y. Song, Sensors Actuators B Chem. **321**, 128498 (2020).
12. A. Salmanipour and M. A. Taher, J. Solid State Electrochem. **15**, 2695 (2011).
13. T. Yin, D. Pan, and W. Qin, J. Solid State Electrochem. **16**, 499 (2012).
14. H. F. Alesary, H. K. Ismail, A. F. Khudhair, and M. Q. Mohammed, Orient. J. Chem. **34**, (2018).
15. A. Michalska, A. Gałuszkiewicz, M. Ogonowska, M. Ocypa, and K. Maksymiuk, J. Solid State Electrochem. **8**, 381 (2004).
16. H.F. Alesary, H.K. Ismail, M.Q. Mohammed. H.N. Mohammed, Z.K. Abbas and S. Barton Chem. Pap. **75**,(2021). https://doi.org/10.1007/s11696-020-01477-8
17. H.K Ismail, H.F Alesary, M.Q Mohammed. J Polym Res. **26**, 65 (2019)
18. G. Bidan, Sensors Actuators B Chem. **6**, 45 (1992).

19. Y. Sun, H. Du, Y. Deng, Y. Lan, and C. Feng, J. Solid State Electrochem. **20**, 105 (2016).
20. M. Q. Mohammed, Thesis, University of Leicester, 2018.
21. M. M. Barsan, M. E. Ghica, and C. M. A. Brett, Anal. Chim. Acta **881**, 1 (2015).
22. G. K. Raghu, S. Sampath, and M. Pandurangappa, J. Solid State Electrochem. **16**, 1953 (2012).
23. M.Q Mohammed, A.M Jassem, J.M Al-Shawi, and H.F. Alesary. AIP Conf Proc. **2290**, 030029 (2020)
24. J. Wang, C. Bian, J. Tong, J. Sun, and S. Xia, Electroanalysis **24**, 1783 (2012).
25. R. K. Shervedani and Z. Akrami, Biosens. Bioelectron. **39**, 31 (2013).
26. M. Vilas-Boas, C. Freire, B. De Castro, and A. R. Hillman, J. Phys. Chem. B **102**, 8533 (1998).
27. A. M. Etorki, A. Robert Hillman, K. S. Ryder, and A. Glidle, J. Electroanal. Chem. **599**, 275 (2007).
28. A. R. Guadalupe and H. D. Abruna, Anal. Chem. **57**, 142 (1985).
29. T. Darmanin and F. Guittard, Soft Matter **9**, 5982 (2013).
30. F.A Almashal, M.Q Mohammed, Q.MA Hassan, C.A Emshary, H.A Sultan, A.M Dhumad, Opt Mater (Amst) **100**,109703 (2020).
31. A. Schultheiss, MN. Gueye, A. Carella, A. Benayad, S. Pouget, J. Faure-Vincent, R. Demadrille, A. Revaux, JP. Simonato, ACS Appl Polym Mater 2:2686 (2020).
32. H. K. Ismail, H. F. Alesary, A. Y. M. Al-Murshedi, and J. H. Kareem, J. Solid State Electrochem. **23**, 3107 (2019).
33. A. R. Hillman, K. S. Ryder, H. K. Ismail, A. Unal, and A. Voorhaar, Faraday Discuss. **199**, 75 (2017).
34. R. M. Sapstead, N. Corden, and A. R. Hillman, Electrochim. Acta **162**, 119 (2015).
35. Y. Lattach, N. Fourati, C. Zerrouki, J.-M. Fougnion, F. Garnier, C. Pernelle, and S. Remita, Electrochim. Acta **73**, 36 (2012).
36. R. M. Brown and A. R. Hillman, Phys. Chem. Chem. Phys. **14**, 8653 (2012).
37. L. Ouyang, B. Wei, C. Kuo, S. Pathak, B. Farrell, and D. C. Martin, Sci. Adv. **3**, e1600448 (2017).
38. M. A. Deshmukh, R. Celiesiute, A. Ramanaviciene, M. D. Shirsat, and A. Ramanavicius, Electrochim. Acta **259**, 930 (2018).
39. L. Niu, C. Kvarnström, K. Fröberg, and A. Ivaska, Synth. Met. **122**, 425 (2001).
40. K. M. Hassan, S. E. Gaber, M. F. Altahan, and M. A. Azzem, Electroanalysis **30**, 1155 (2018).
41. S. K. Pandey, S. Sachan, and S. K. Singh, Mater. Sci. Energy Technol. **2**, 667 (2019).
42. Y. Zhang, C. Li, Y. Su, W. Mu, and X. Han, Inorg. Chem. Commun. **111**, 107672 (2020).
43. H. Fourou, A. Zazoua, M. Braiek, and N. Jaffrezic-Renault, Int. J. Environ. Anal. Chem. **96**, 872 (2016).
44. Z. Zhai, N. Huang, H. Zhuang, L. Liu, B. Yang, C. Wang, Z. Gai, F. Guo, Z. Li, and X. Jiang, Appl. Surf. Sci. **457**, 1192 (2018).
45. V. H. Dang, P. T. H. Yen, N. Q. Giao, P. H. Phong, V. T. T. Ha, P. K. Duy, and C. Hoeil, Electroanalysis **30**, 2222 (2018).
46. K. M. Hassan, G. M. Elhaddad, and M. AbdelAzzem, Microchim. Acta **186**, 440 (2019).

47. D. Qin, S. Gao, L. Wang, H. Shen, N. Yalikun, P. Sukhrobov, T. Wagberg, Y. Zhao, X. Mamat, and G. Hu, Microchim. Acta **184**, 2759 (2017).
48. F. L. Migliorini, R. C. Sanfelice, A. Pavinatto, J. Steffens, C. Steffens, and D. S. Correa, Microchim. Acta **184**, 1077 (2017).
49. R. Manikandan and S. S. Narayanan, Ionics (Kiel). **25**, 6083 (2019).
50. N. Promphet, P. Rattanarat, R. Rangkupan, O. Chailapakul, and N. Rodthongkum, Sensors Actuators B Chem. **207**, 526 (2015).
51. H. D. Vu, L.-H. Nguyen, T. D. Nguyen, H. B. Nguyen, and T. L. Nguyen, Ionics (Kiel). **21**, 571 (2015).

Figures

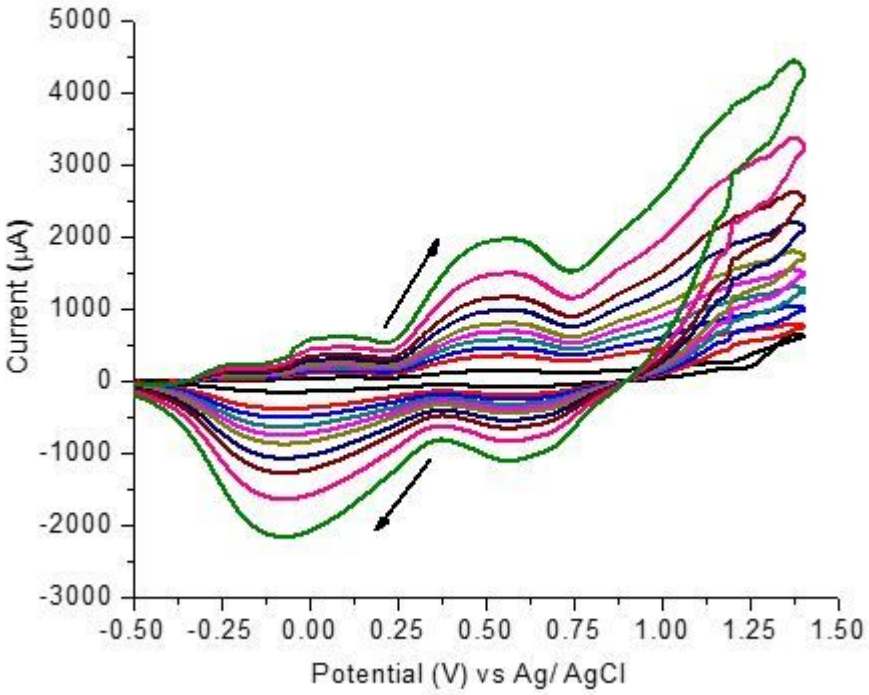

Figure 1

Cyclic voltammogram resulting from electropolymerisation of 10 mM EDOT/Schiff base with 0.1 M Bu4NPF6 in DCM solution between 0.5 and 1.4 V at 10 mV s-1 for 10 scans. Electrode area was 0.00785 cm2.

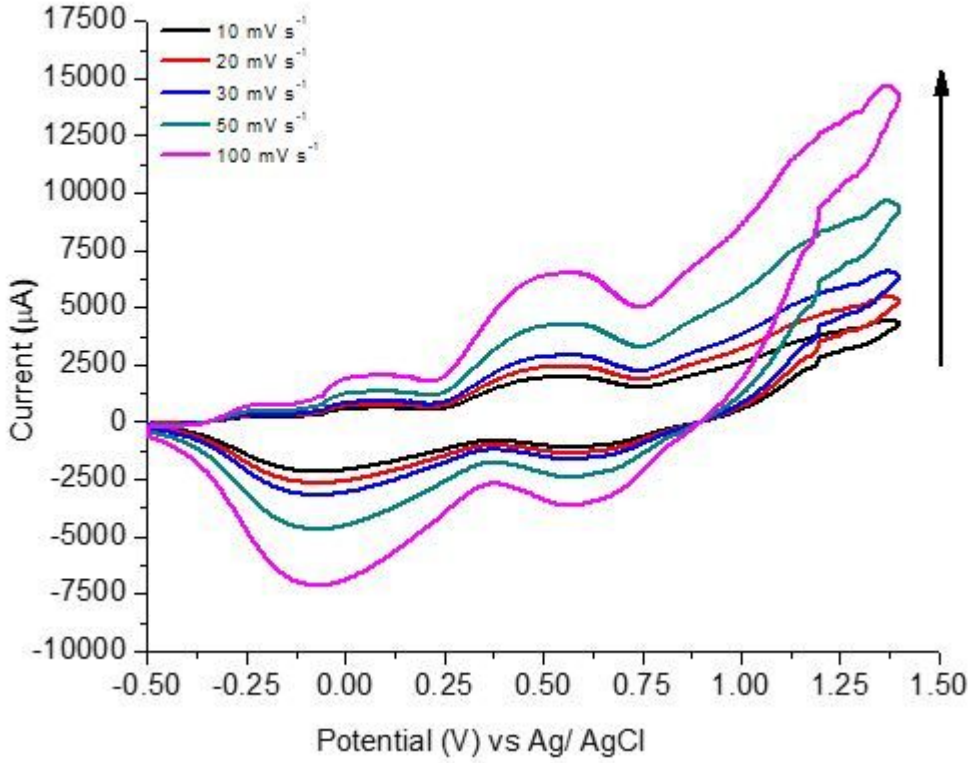

Figure 2

Cyclic voltammogram (scan 10) for deposition of 10 mM EDOT/Schiff base with 0.1 M Bu4NPF6 in DCM solution at different scan rates, v, 5-100 mV s-1. Electrode area was 0.00785 cm2.

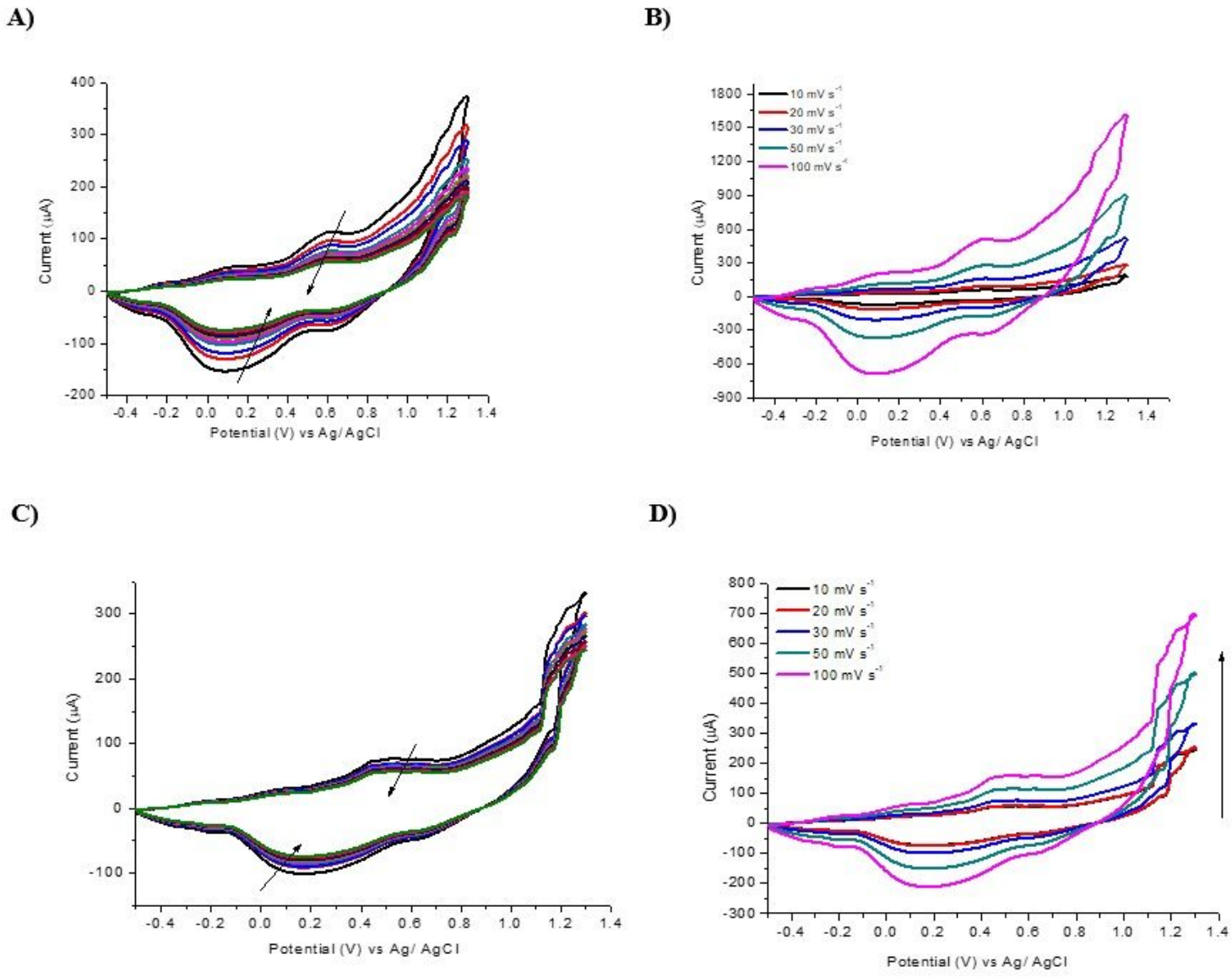

Figure 3

Voltammetric response of poly(EDOT/Schiff) electrodes prepared at 10 mV s-1 (Figure 1) and acquired in A) 0.1 M Bu4NPF6 in DCM and C) 0.1 M Bu4NPF6 in the aqueous electrolyte (monomer-free) at 0.5 to 1.3 V. Voltammetric responses of the same polymer film at various scan rates ranging over 10-100 mV s-1 B) DCM and D) aqueous electrolyte.

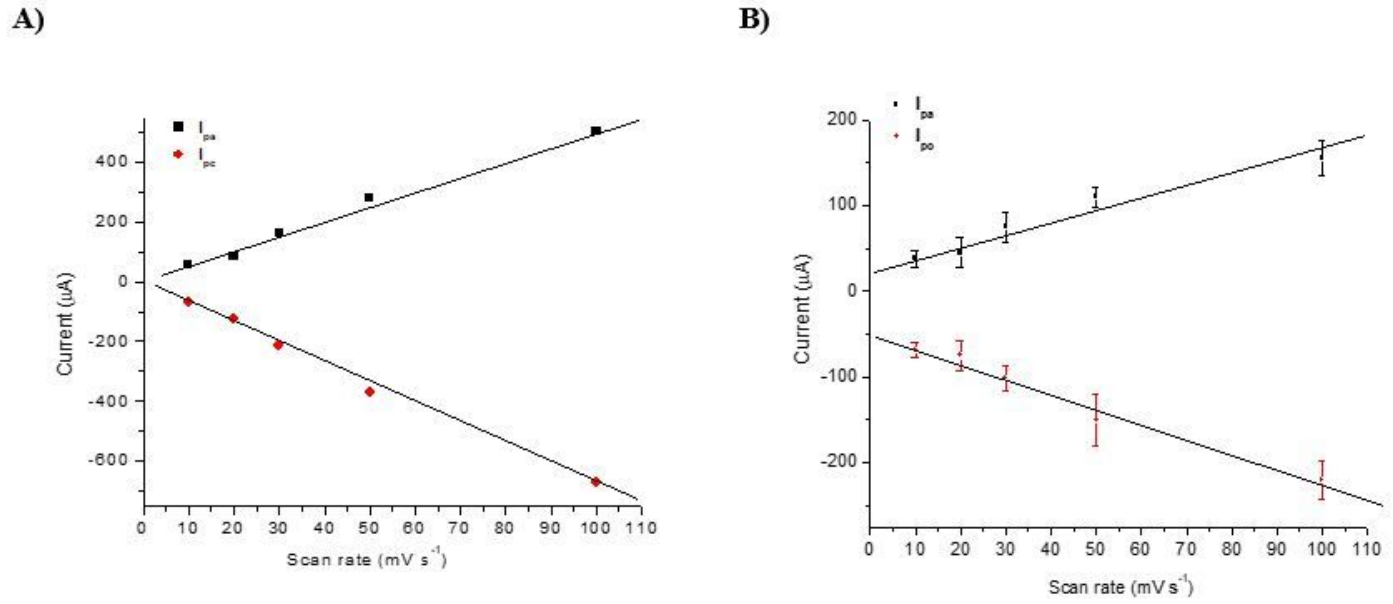

Figure 4

Variation of redox peak current A) from Figs. 3B and B) from Fig. 3D with different scan rates 10-100 mV s-1.

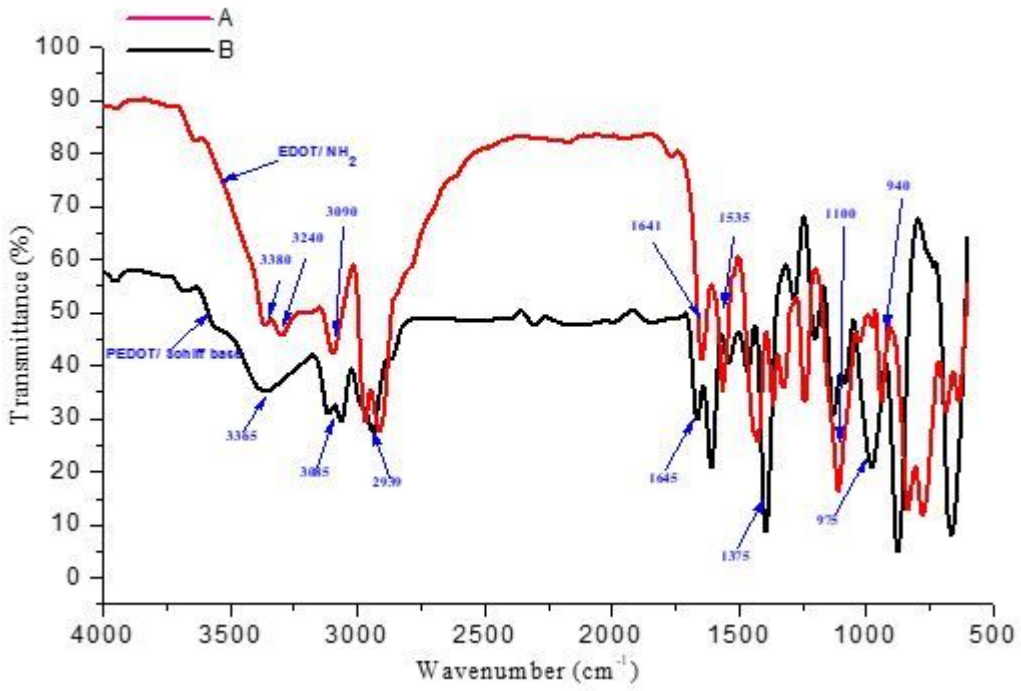

Figure 5

FTIR spectra of A) synthesized monomer (red line) and B) synthesized poly(EDIT/Schiff base) (black line).

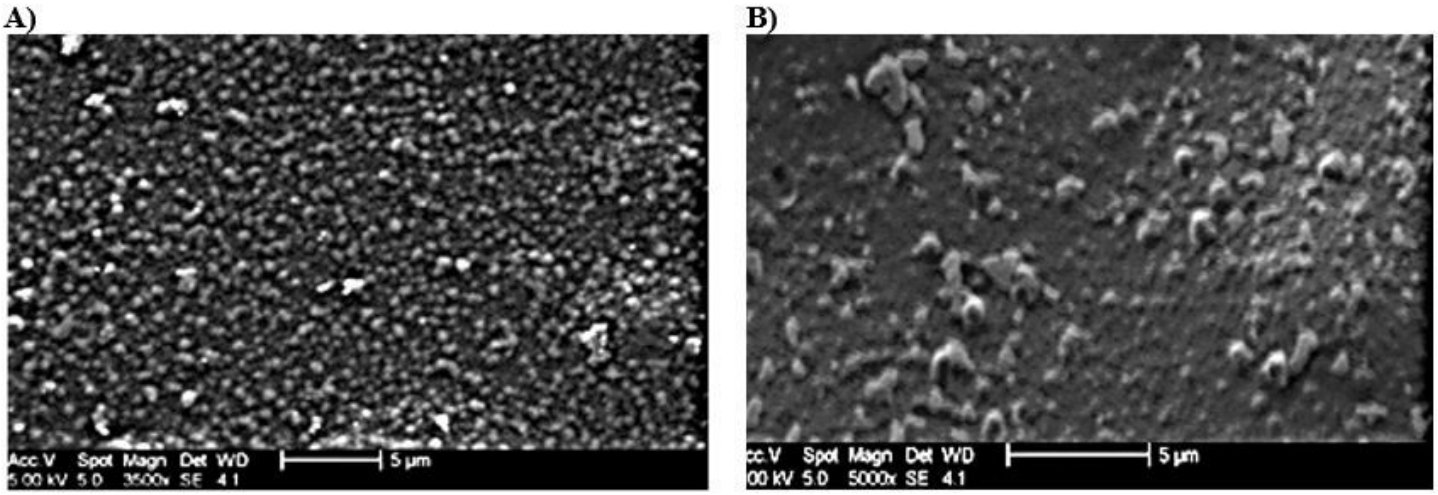

Figure 6

SEM images for the poly(EDOT/Schiff) surfaces formed using electropolymerization by different scan rates A, 10, and B, 100 mV s-1.

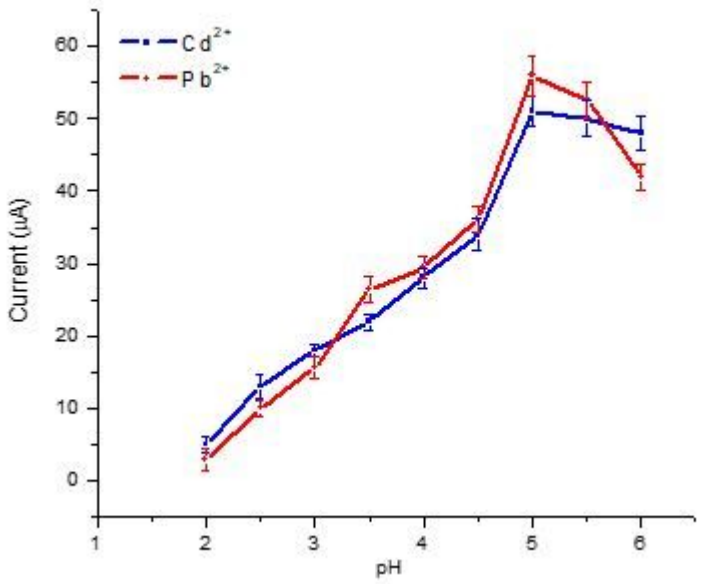

Figure 7

Plot of SWV peak currents for Cd and Pb ions as a function of pH as obtained on PEDOT/Schiff electrodes.

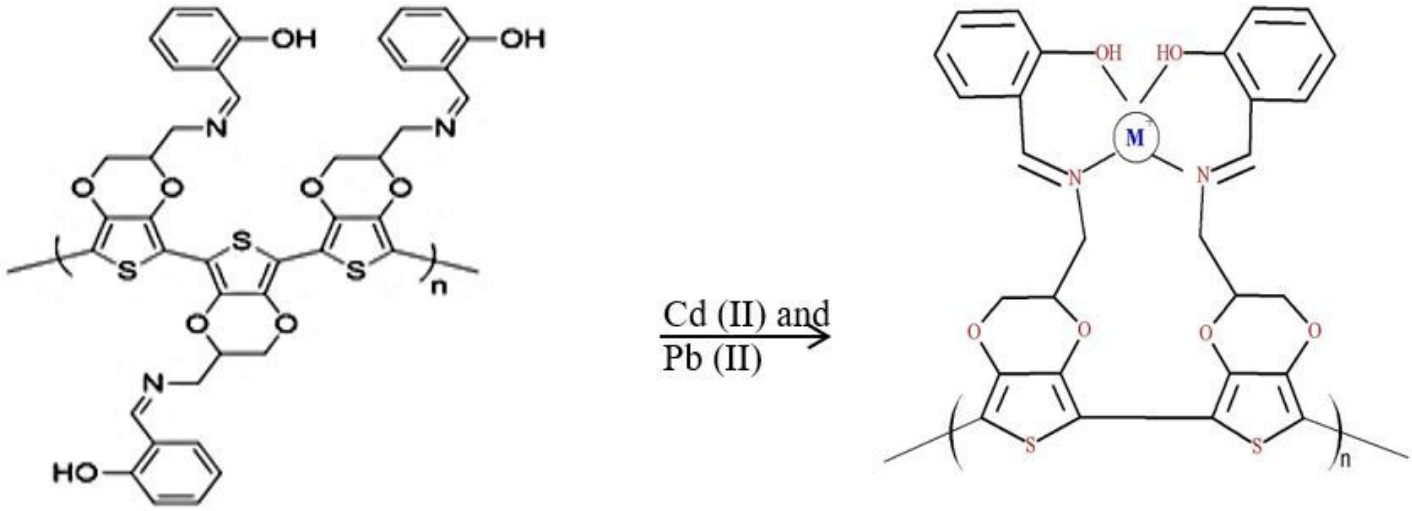

Figure 8

Assumed schematic for the formation of the PEDOT/Schiff-metal ion complexes.

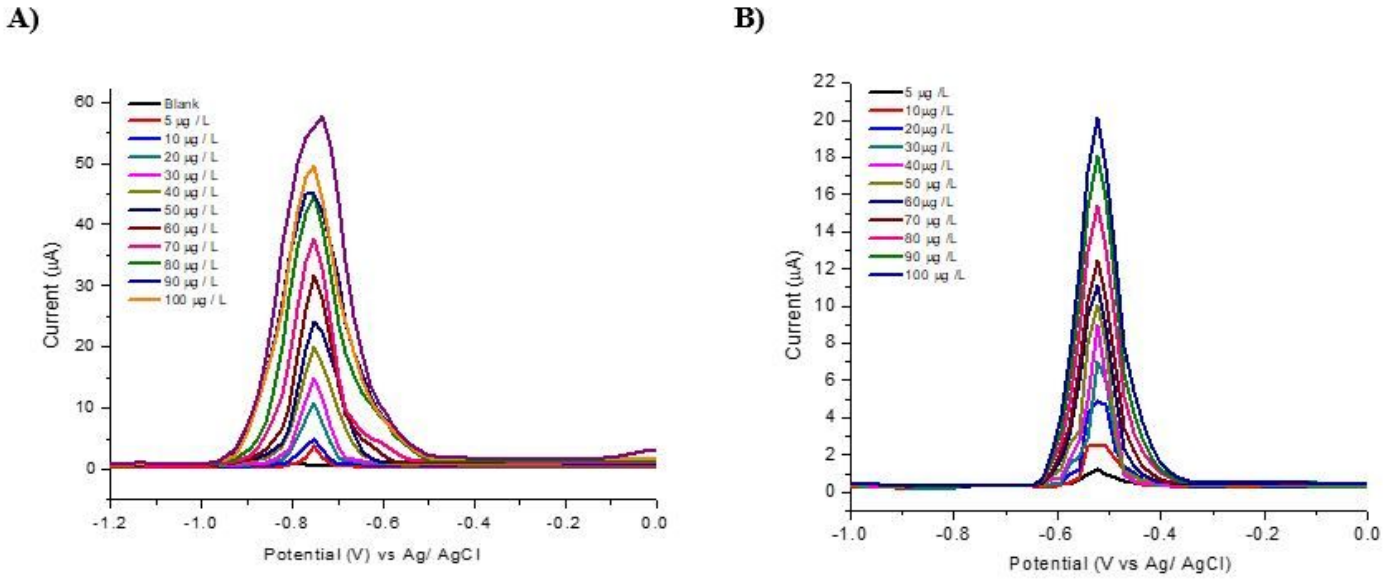

Figure 9

SWV curves for different concentrations of (A) Cd (II) and (B) Pb (II) from lower to higher concentration (5-100 µg L-1) using a poly(EDOT/Schiff) electrode.

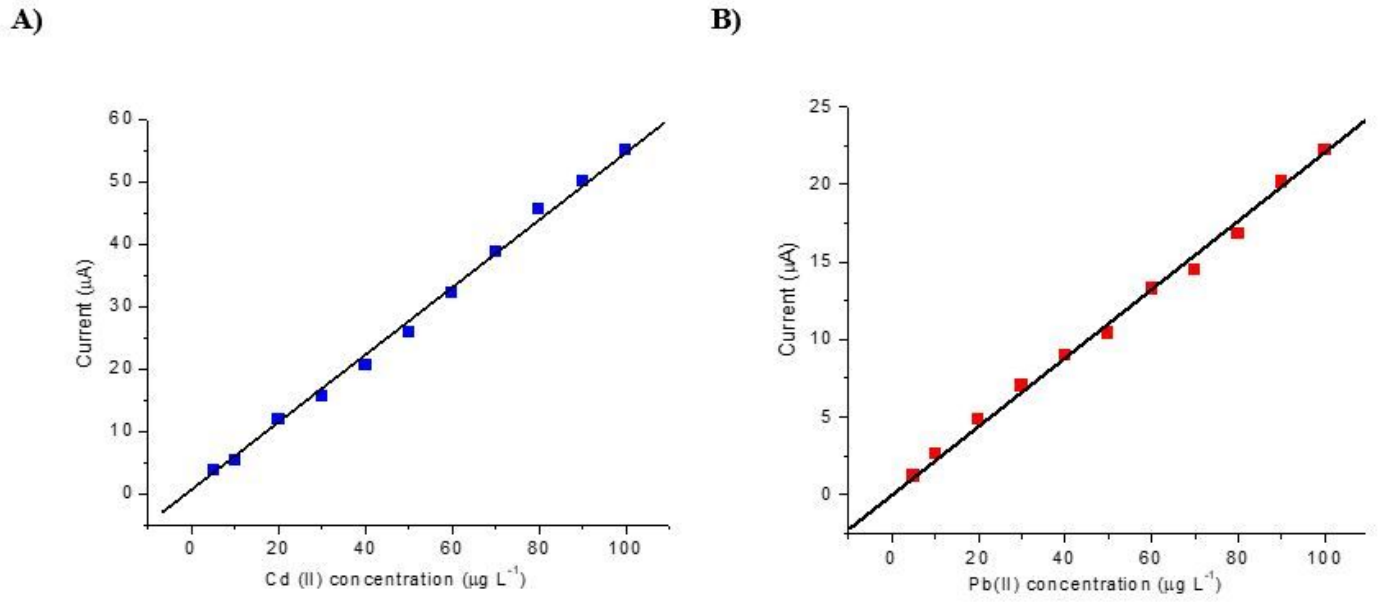

Figure 10

Calibration plot for measurement of different concentrations (5-100 µg L-1) of (A) Cd (II) and (B) Pb (II) from Fig. 9 using a poly(EDOT/ Schiff) electrode.

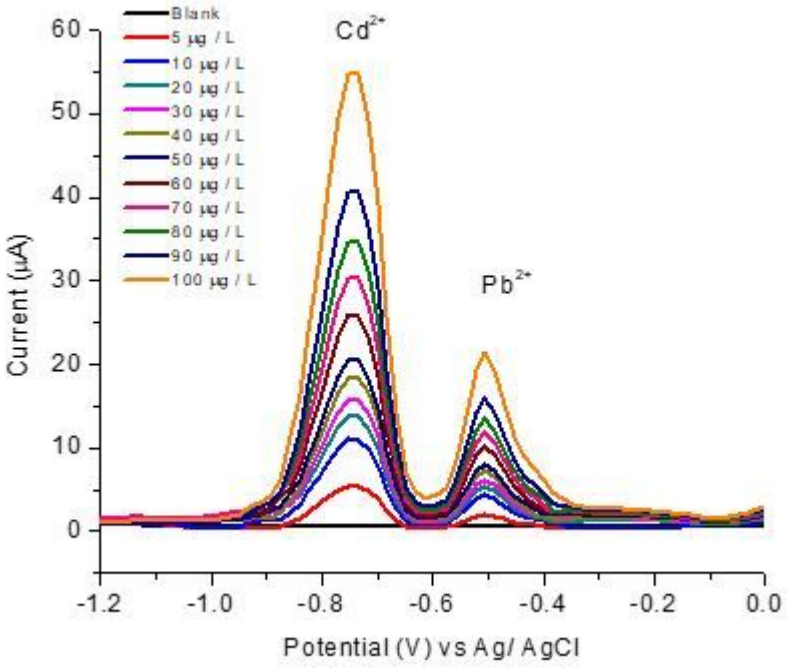

Figure 11

SWV response of poly(EDOT/Schiff) electrode for the simultaneous analysis of Cd (II) and Pb (II).

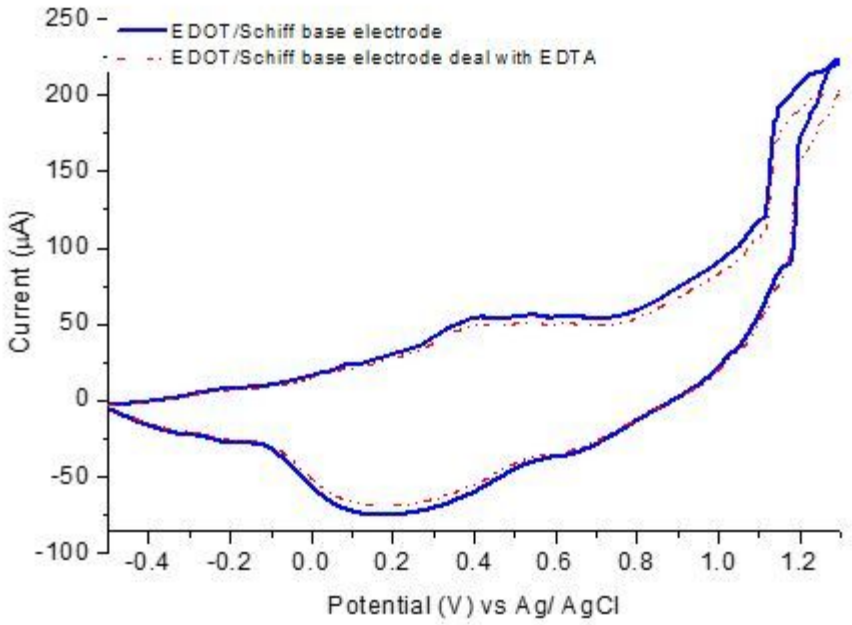

Figure 12

Cyclic voltammetric of PEDOT/Schiff modified electrode, blue curve) in Bu4NPF6 aqueous electrolyte, red curve) after treating with 0.1 M EDTA

Supplementary Files

This is a list of supplementary files associated with this preprint. Click to download.

- Graphicalabstract.docx
- formulas.docx